

Leo P. Kadanoff

Hydrodynamic systems often show an extremely complicated and apparently erratic flow pattern of the sort shown in figure 1. These turbulent flows are so highly time-dependent that local measurements of any quantity that describes the flow—one component of the velocity, say—would show a very chaotic behavior. However, there is also an underlying regularity in which the motion can be analyzed (see figure 1 again) as a series of large swirls containing smaller swirls, and so forth. One approach to understanding this turbulence is to ask how it arises. If one puts a body in a stream of a fluid—for example, a piece of a bridge sitting in the

stream of a river—then for very low speeds (figure 2a) the fluid flows in a regular and time-independent fashion, what is called laminar flow.¹ As the speed is increased (figure 2b), the motion gains swirls but remains time-independent. Then, as the velocity increases still further, the swirls may break away and start moving downstream. This induces a time-dependent flow pattern—as viewed from the bridge. The velocity measured at a point downstream from the bridge gains a periodic time-dependence like that shown in figure 2c. The parameter that characterizes these changes in the flow pattern is the dimensionless Reynolds number \mathcal{R} , which is the product of the velocity and density times a characteristic length (the size of the bridge pier, for example) divided by the viscosity. As \mathcal{R} is increased still further, the swirls begin to induce irregular internal swirls as in the flow pattern of figure 2d. In this case, there is a partially periodic and partially irregular velocity history

(see the second column of figure 2d). Raise \mathcal{R} still further and a very complex velocity field is induced, and the $v(t)$ looks completely chaotic as in figure 2e. The flow shown in figure 1 has this character.

These different flow patterns can also be characterized by looking at the power spectrum of the flow. The power spectrum $P(\omega)$ is the square of the Fourier transform of the velocity field:

$$\hat{V}(\omega) = \frac{1}{\sqrt{T}} \int_0^T dt e^{2\pi i \omega t} v(t)$$

$$P(\omega) = |\hat{V}(\omega)|^2$$

The fourth column of figure 2 shows the power spectra for the flow patterns we've discussed. For the time-independent flows, figures 2a and 2b, $P(\omega)$ shows a spike at zero frequency. In the periodic region (figure 2c), additional spikes appear at the frequency of the oscillation and at its harmonics, that is, at integer multiples of this frequency. As the motion becomes partially chaotic

Leo Kadanoff is professor of physics at the University of Chicago and a member of the James Franck and Enrico Fermi Institutes there.

Simple mathematical systems exhibit complex patterns of behavior that can serve as models for chaotic behavior, including perhaps turbulent flow in real hydrodynamic systems.

tic, as in figure 2d, a broad, slowly varying background appears behind the spectral lines. Finally, the fully chaotic flow has a power spectrum that is apparently continuous.

We would, of course, like to understand this transition to turbulence in hydrodynamical systems. Unfortunately, after many years of study by scientists in many different disciplines, we still do not have a fully satisfactory approach to this problem. In this article, I would like to describe an extremely simplified model that shows a kind of transition to chaos and to discuss how the features of this model can be, and have been, observed in hydrodynamic systems.

The spirit of this approach is similar to the one used in the theory of critical phenomena in condensed-matter physics: To understand a complicated phase transition—that is, a change in behavior of a many-particle system—choose a very simple system that shows a qualitatively similar change. Study this simple system in detail. Abstract those features of the behavior of the simple system that are “universal”—that is, appear to be independent of the details of the system’s makeup. Apply these universal features to the more complex problem.

Our simple problem is so simple that one might, at first glance, imagine that it contains nothing of interest. But it has an amazingly intricate and regular structure. Consider a dynamical system characterized by one variable, x . At time zero, the value of this variable is x_0 ; at discrete later times $t = j\tau$ it has the value x_j . The major assumption is that the value of the variable at one step x_j determines the value at the next. Mathematically we write

$$x_{j+1} = R(x_j) \quad (1)$$

where $R(x)$ is a function that describes the dynamics. Our job is to find time histories of the system.² That is, we start from x_0 , find $x_1 = R(x_0)$, $x_2 = R(x_1)$ and so forth; we then look for patterns in the sequence x_0, x_1, x_2, \dots . One simple visualizable model for such a system is an island containing an insect population which breeds in the summer and leaves eggs that hatch the next summer; our variable is the population each summer. Specifically, x_j is the ratio of the actual population in the

summer of the j th year to some reference population. To make our model explicit, we assume that the population next summer x_{j+1} is determined by the population this summer via the relation

$$x_{j+1} = rx_j - sx_j^2$$

Here there are two terms. The first term rx_j represents the natural growth rate of the population; the term sx_j^2 represents a reduction of this natural growth caused by overcrowding of the insects. When r is greater than 1, the first term simply expresses an increase in the population by a factor r in each year. If this were the only term, the population would grow exponentially. The second term represents the reduction in the population growth caused by, for example, competition for resources (or perhaps shyness) of the insects when the population is large. By rescaling, that is, by letting x_j be replaced by $(r/s)x_j$, one can convert this equation into a standard form:

$$x_{j+1} = rx_j(1 - x_j) \quad (2)$$

We wish to examine the long-term behavior of the population, or of x_j , based upon equation 2. In particular, we are interested in how this behavior depends upon the growth rate r . We can think of r as being akin to the Reynolds number in the hydrodynamic example. To keep the insect population ratio in the interval between 0 and 1 we limit our examination to values of r between 0 and 4.

First we study the behavior for small r . If r is less than 1, the insects are living in such an inhospitable environment that their population will diminish each year. Their population pattern is like that shown in figure 3a. If, for example, $r = 1/2$ and one starts from $x_0 = 1/2$, then x_1 is $1/8$ and each succeeding x_j is less than $2^{-(j+2)}$. The population simply dies away to zero, for all starting values. This result is summarized in figure 4 in which we plot eventual population values as a function of r . For values of r below 1, the eventual population is zero. Roughly speaking, we might think of this behavior as akin to the laminar (smooth) flow in figure 2a.

The region of r between 1 and 3 shows another kind of simple behavior,

perhaps akin to the time-independent swirls of figure 2b. If we start with any x_0 between zero and one, the population approaches a constant but non-zero value. This constant population, x^* can be found by replacing both x_j and x_{j+1} in equation 2 by x^* :

$$x^* = rx^*(1 - x^*)$$

which has the two solutions $x^* = 0$ and

$$x^* = 1 - 1/r \quad (3)$$

Such a self-generating value of x is called a fixed point. The zero-population solution is unstable. If we start with a very low population (see figure 3b), the population will increase year by year until it settles down to the value given in equation 3. The final populations $1 - 1/r$ are also plotted in figure 4. This behavior might be considered to be compatible with the time-dependent flow of figure 2b.

Thus the region in which r is below 3 is easily understood. No chaos has arisen so far. Now jump to $r = 4$. Figure 3c shows the values of x induced at this value of r , starting from $x_0 = 0.707$. Apparently the population x_j assumes all values of x in the range between zero and one starting from this point. Although x_{j+n} is uniquely determined by x_j , for large n the pattern of determination looks chaotic rather than—as it is—deterministic. For small n , one can see patterns (for example, that small x_j produces small x_{j+1}) but these correlations become invisible as $n \rightarrow \infty$. What we see is apparent chaos.

For $r = 4$ (only!) one can solve equation 2 by the simple change of variables

$$x_j = (1 - \cos 2\pi\theta_j)/2$$

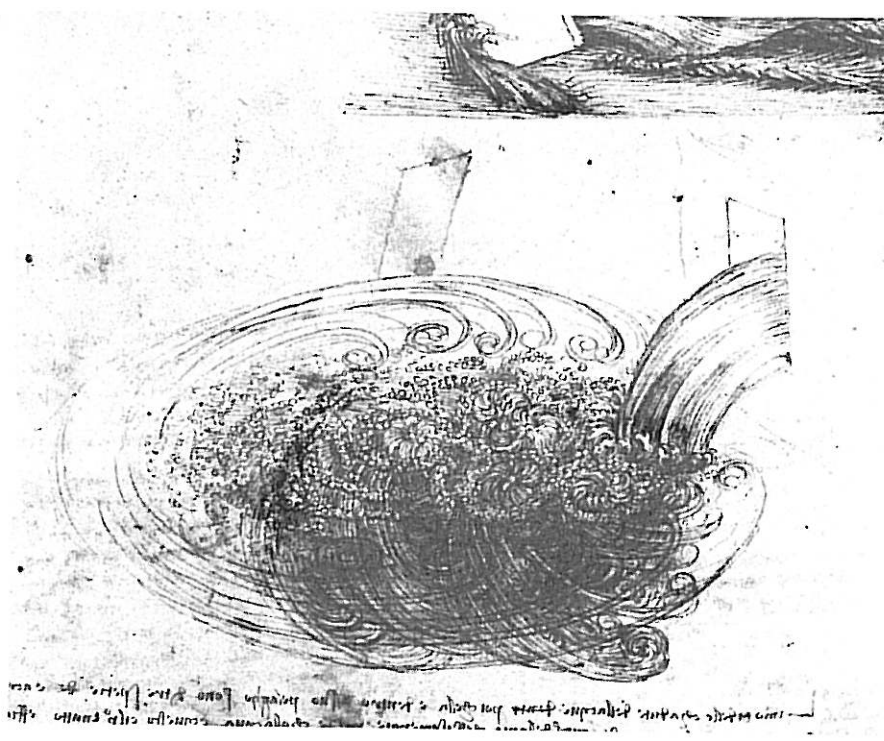
Then equation 2 can be converted into the statement

$$\begin{aligned} \frac{1}{2}(1 - \cos 2\pi\theta_{j+1}) &= 4[\frac{1}{2}(1 - \cos 2\pi\theta_j)] \\ &\times [\frac{1}{2}(1 + \cos 2\pi\theta_j)] \\ &= \frac{1}{2}(1 - \cos 4\pi\theta_j) \end{aligned}$$

which has as one solution $\theta_{j+1} = 2\theta_j$ or

$$\theta_j = 2^j\theta_0 \quad (4)$$

One can see the chaos in the solution quite directly. Since x_j is related to $\cos 2\pi\theta_j$, adding an integer to θ_j (or changing its sign) leads to the very



Turbulent flow patterns as drawn by Leonardo da Vinci. Note how the large swirls break into smaller ones, and these again break up. (From the Royal Library, Windsor Castle; reproduced with permission.)

Figure 1

same x_j . Hence if one writes θ_j in ordinary base-10 notation as, say, $\theta_j = 11.2693 \dots$ one can simply throw away the 11. Better yet, if one writes θ_0 as a "decimal" base 2, as for example

$$\theta_0 = \frac{1}{2} + \frac{1}{8} + \frac{1}{16} + \frac{1}{64} + \dots \\ = 0.101101 \dots$$

then the multiplication by 2 is simply a shift in the "decimal" point, so that

$$\begin{aligned} \theta_1 &= .01101 \dots \\ \theta_2 &= .1101 \dots \\ \theta_3 &= .101 \dots \\ \theta_4 &= .01 \dots \end{aligned}$$

Thus, if we start out with any θ_0 , the θ_j produced will depend on the j th and higher digits in θ_0 . This gives us one possible definition of chaos: For large j the dynamical variable x_j has a value which is extremely sensitive to the exact value of x_0 . In our case, suppose we have two starting values x_0 and x'_0 that differ by a small number ϵ and generate two sequences of populations x_j and x'_j based, respectively, upon x_0 and x'_0 , then after j steps, the difference grows to the value $2^j \epsilon$. (See also

Joseph Ford's article, "How random is a coin toss?" April, page 40.)

In fact, the calculation represented in the picture of Figure 3c is, in some sense, incorrect. It was calculated on a computer with 16 decimal digits. After

about 50 steps, an initial error of 10^{-16} grows to be an inaccuracy of order 1. Consequently, all the points after step 50 are wrong, representing some random effect in the computer, and not a selected initial value.

This might be an appropriate point to mention that one of the major sources of modern stochastic theory is the work of the meteorologist Edward Lorenz.³ As an analog to weather forecasting, he studied systems like our $r = 4$ system, in which the final state is an extremely sensitive function of the initial state. For this kind of system, as the prediction period grows longer, both the initial data needs and the computational power required grow exponentially. True long-range detailed weather prediction is, in practical terms, impossible.

The system at $r = 4$ is chaotic in another sense. For almost any randomly chosen x_0 —or θ_0 —the set of resulting θ_j will be uniformly distributed between 0 and 1. Correspondingly, we will get a set of x_j 's in which the probability $p(y)$ that x_j will have the value between y and $y + dy$ is proportional to $(y(1-y))^{-1/2}$ for almost any starting point. Thus the time average for this chaotic system is the same for almost every starting point.

We have inserted on the right-hand side of figure 4 this distribution for this value of r by showing all x between 0

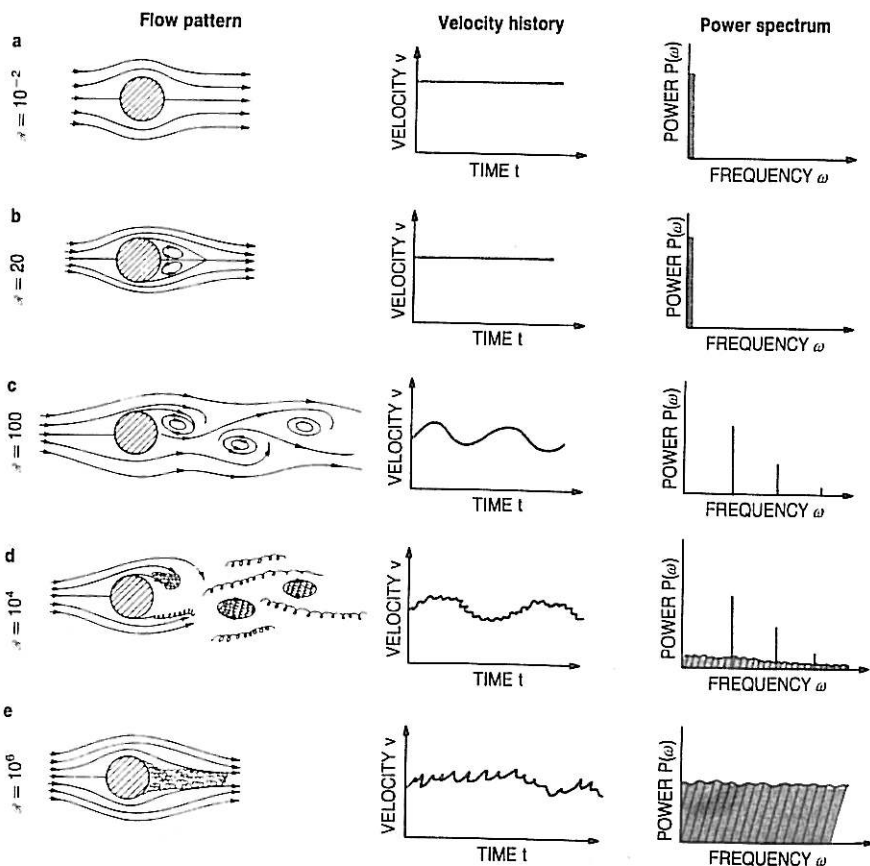


Figure 2

Patterns of hydrodynamic flow for various Reynolds numbers R . At small values of R the flow is laminar (a); as R is increased, the flow becomes first periodically undulating (c) and finally turbulent (e). In the graphs for each Reynolds number, we plot the time variation of one component of the velocity as measured, for example, at the indicated point in the sketches; we also show the power spectrum $P(\omega)$ for these time variations of the velocity.

and 1 as possible long-term values.

A final definition of chaos is that the power spectrum

$$P(\omega) = \frac{1}{N} \left| \sum_{j=1}^N x_j e^{2\pi i \omega_j} \right|^2 \quad (5)$$

has broad spectral features. For $r = 4$ and large N , the power spectrum can be calculated exactly. For almost any x_0 it is perfectly flat.

There are some special values for x_0 that generate exceptional patterns of x_j . We can see these patterns more readily if we first note that one can always choose θ_j to be in the interval between 0 and $1/2$, because θ_j can be flipped in sign and shifted by an integer without changing x_j . Thus, the recursion relation for θ_j can be written as

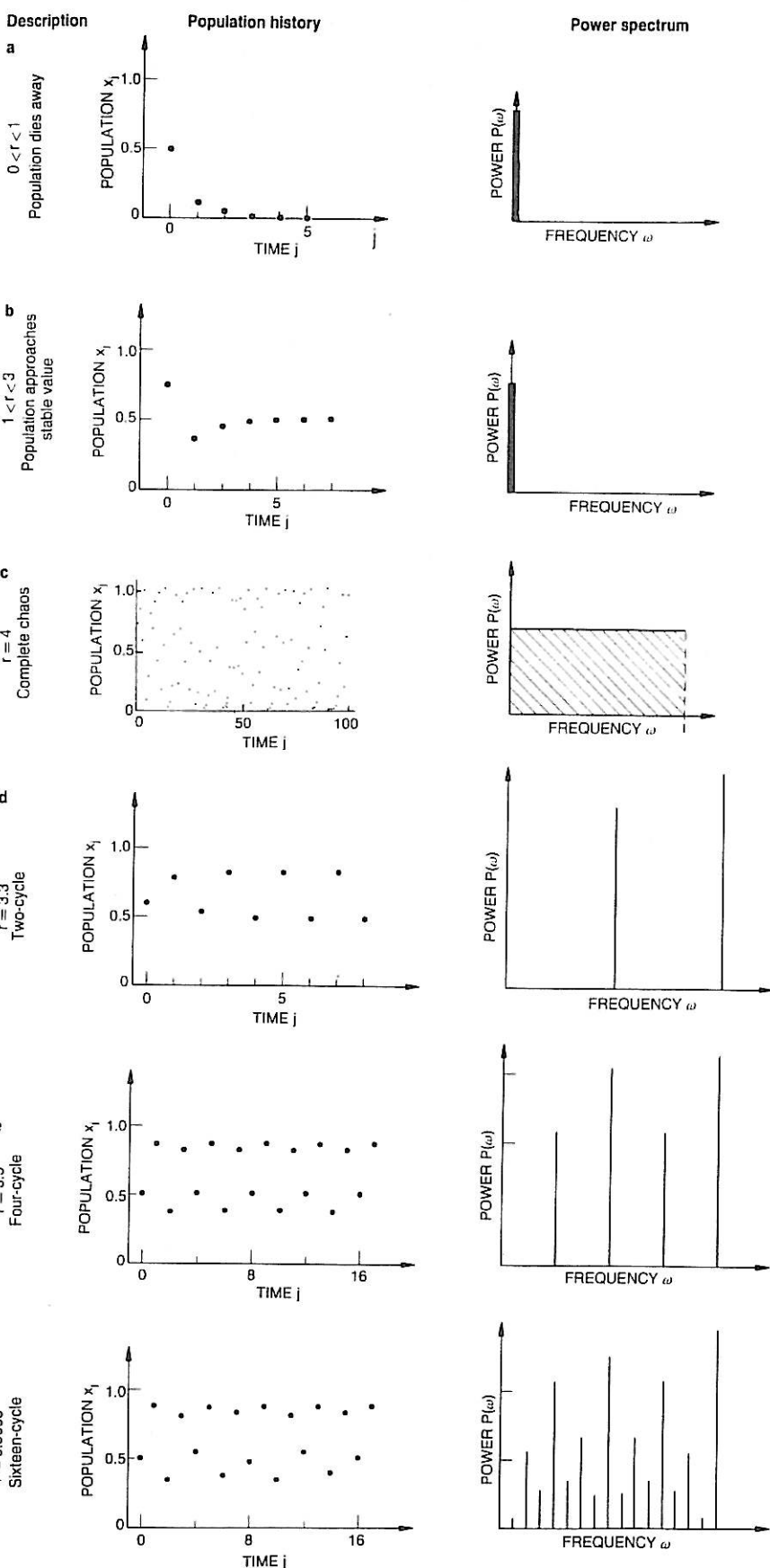
$$\theta_{j+1} = \begin{cases} 2\theta_j & \text{for } 0 \leq \theta_j < 1/4 \\ 1 - 2\theta_j & \text{for } 1/4 \leq \theta_j < 1/2 \end{cases} \quad (6)$$

Any rational number that is chosen for θ_0 will lead to a recurring pattern of θ_j and x_j . For example, if we take $\theta_0 = 1/3$ then all subsequent θ_j are also $1/3$, so this is a fixed point. If one starts with $\theta_0 = 1/5$ then the subsequent θ_j are $2/5, 1/5, 2/5, 1/5$ and so forth. Thus we have a cyclic behavior with a period of length 2. One solution that has period of 3 is $1/2, 2/9, 4/9$. Equation 6 has periodic solutions with all possible periods.⁴

Now we have long-term solutions for equation 3 that are time-independent for r between 0 and 3 and one that is quite chaotic for $r = 4$. Next, increase r from 3 and observe the first hints of chaos which arise. As r increases just above 3 the fixed point at x^* near $2/3$ becomes unstable; instead, the population keeps flipping back and forth between high and low values. The insects start from a low population. They reproduce avidly, leaving a large number of eggs. But the resulting population next year is too crowded (or shy), so the population the year after will be low. Thus, odd years will have high populations, even years low populations. The Bible records⁵ that Joseph predicted such a periodic behavior with a basic time step of seven years. In our model the exact values of x for the two-cycles are

$$x = \frac{1}{2}(1 + 1/r) \pm \frac{1}{2}[(1 + 1/r)(1 - 3/r)]^{1/2}$$

These $q = 2$ cycles remain stable over the range of r between 3 and $1 + \sqrt{6} = 3.4495$. I will call this upper value of r at which the two-cycle becomes unstable r_2 . For r slightly larger than r_2 , the stable behavior is a four-cycle, as shown in figure 3e. The basic period of the behavior has doubled once more. This behavior is also only stable up to a limiting value, r_4 . Above r_4 an eight-cycle appears and remains stable between r_4 and r_8 , whereupon a sixteen-cycle appears. These stable beha-



Behavior of a population that obeys a simple nonlinear reproduction equation (see the text). We show both the time evolution and the corresponding power spectrum of the population for various values of the growth parameter r . For growth parameters above 3.0, no stable population is reached; in the cases shown here the population oscillates over a varying number of cycles. The oscillations show up as peaks in the power spectrum, with each higher-order cycle contributing less than the earlier cycles.

Figure 3

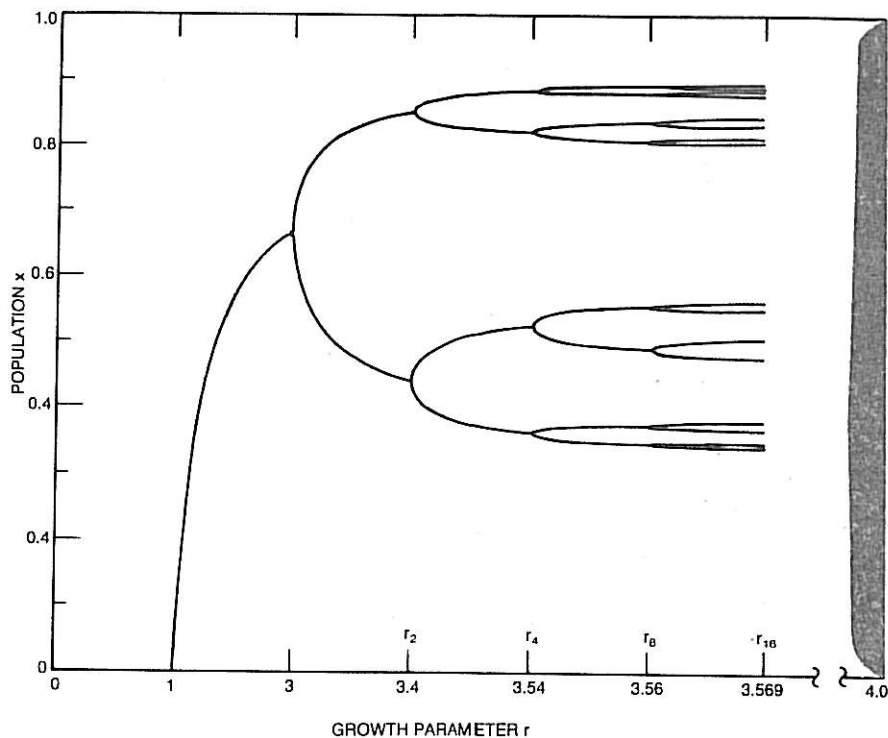
vior is shown on figure 4 as doublings in the number of x -values which the system assumes as j becomes infinite. Successive doublings continue until at $r_c = 3.569 \dots$, when a cycle of infinite length appears.

To see the beginnings of the onset of chaos in this model, look at the power spectrum defined by equation 5. When the fixed point is the stable behavior, the power spectrum is a spike at zero frequency. When the two-cycle appears, another frequency, $\omega = 1/2$, appears in the spectrum, as figure 3d shows. This frequency is, of course, equal to the inverse period of the motion. Between r_2 and r_4 , $\omega = 1/4$ and $\omega = 3/4$ also enter, as in figure 3e. As the period increases, more and more spectral lines enter until at r_c there are infinitely many lines.

Of course, a spectrum with an infinite number of discrete lines is not the same as a broad-band, continuous spectrum. Even at $r = r_c$ there is no fully developed chaos of the type that occurs at $r = 4$. However, in this model, the development of an infinite number of lines through successive period doublings is a major step toward the production of chaos.

To see the remaining steps, turn to figure 5. This picture is, like figure 4, a depiction of the populations that arise after a huge number of iterations of an initial x_0 . Our job is to understand how this picture changes between r_c and 4. We shall discuss the predominant features of this development, leaving out for the moment small regions—which appear as white stripes in the more or less uniformly gray area—in which stable cycles once again dominate the picture.

We start at $r = 4$ and decrease r . As we saw, an initial x_0 generates points that move erratically through an entire band of permitted x -values. As r decreases, this band narrows slightly to be between $r(1 - r/4)$ and $r/4$, but the behavior is otherwise qualitatively unchanged. The spectrum contains no sharp peaks. However, below the value labeled r_2' the behavior changes. The band splits into two. Between r_2' and r_4' , the population is somewhere in the lower band on even steps; on odd steps it lies somewhere in the upper. The spectrum then has a broad background produced by the erratic values the population assumes in each band and a sharp peak at $\omega = 1/2$ produced by the regular way it jumps from band to band. Then at r_4' the behavior changes once more. There are four bands, which we can number from bottom to top as 1, 2, 3, 4, and the motion goes from band 1 to 3 to 2 to 4—which is, not accidentally, exactly the same ordering as the motion in the four-cycle. As r decreases beyond r_8' there are eight bands, then beyond r_{16}' sixteen, and so



Stable values for the population as a function of the growth parameter r . The solid lines show the values of the population x_j that recur as j becomes infinite. For growth parameters r below 1, the population decays to 0. For r between 1 and 3.4, there is no single stable value—instead the population oscillates between the two values in the upper and lower branches of the curve. Above 3.54, the population oscillates among the four branches, and so forth. These oscillations give rise to the peaks in the power spectrum shown in figure 2. Note the highly nonlinear scale. Note also the break at 3.569; the subsequent behavior for growth parameters between 3.569 and 4 is shown in figure 5. Here we indicate only the continuum of values allowed as the population approaches the truly chaotic behavior at $r = 4$.

Figure 4

forth. When there are 2^n bands, the population returns to a given band after 2^n steps but the exact point at which it returns is chaotic in exactly the same sense as there is chaos at $r = 4$. In this region of 2^n bands there are sharp spectral lines at 2^{-n} times an integer together with a broad background produced by the erratic behavior in the band. To the naked eye this erratic behavior looks very much the same as the $r = 4$ chaotic motion. The only differences are ones of scale. In this 2^n -band case, the erratic motion is confined to a set of narrow regions, inside each band. Furthermore, the motion only returns to the band every 2^n steps, so that as we change values of r , there is a change in the time-scale as well. (A reader who is acquainted with renormalization and scaling might wonder whether this change of scale might be used to build a renormalization-group analysis of the period-doubling process. It can, and has.⁶)

This process of successive band splittings enables the system to interpolate smoothly between the full chaos at $r = 4$ and the 2^∞ cycle at r_c . As r approaches r_c from above, we get more and more bands until at r_c there are 2^∞ bands, each of them infinitesimally

narrow, and merging into the infinite number of lines just below r_c .

All of this so far has applied to our simple model, given by equation 2. However, it is important to notice that the general nature of the processes of period doubling and band splitting are independent of the details of the model and will occur with any mapping of the form

$$x_{j+1} = r/f(x_j)$$

with $f(0) = f(1)$ and f being a smooth function with a single maximum in the interval 0 to 1.

Furthermore, Mitchell Feigenbaum has looked⁶ at several maps and demonstrated that some of the quantitative properties of the behavior of band splitting and period doubling near r_c —that is, for large numbers of periods—apply equally well to almost all maps with a smooth maximum in which $f''(x)$ is negative at the maximum. In particular recall that r_q and $r_{q'}$ are, respectively, the values of r at which a $q = 2^n$ cycle first appears or $q = 2^n$ bands merge. (Again, refer to figures 4 and 5 for a depiction of these bands and cycles.) As n becomes infinite, these limiting values both approach the same limiting value r_c . Feigenbaum showed

that for large n they approached r_c in a very simple manner, namely:

$$r_q - r_c = A\delta^{-n}$$

$$r_{q'} - r_c = A'\delta^{-n}$$

Here A and A' , naturally, depend in detail upon the mapping function $f(x)$. However, the exciting and surprising result of his work was that δ is universal: It does not change as we change the mapping function f . A similar result is obtained for the splitting of the x_j values. When one chooses in an appropriate fashion two neighboring values for x_j that lie in a 2^n -cycle, one finds that the separation between these values decreases with n as $B\alpha^{-n}$, where α is universally equal to 2.503.... Feigenbaum has also given a renormalization group treatment that verifies this universality and generates the universal numbers δ and α .

If these quantitative results for large n apply to all mathematical maps, might they not also apply to real dynamical systems? In particular, if we use x_t to refer to some dynamical property at time t and let $f(x_t)$ describe how the dynamical property at time t determined its value at time $t + \tau$, will we be able to see the period-doubling behavior our maps show?

Nonlinear electrical circuits have been shown⁷ to give a very similar behavior to the one described above. As a control parameter, r , in the circuit is varied, one of the circuit variables, such as a voltage, traces patterns in which successive period doublings occur. Moreover, the observed values of α and δ are the same as the values mentioned above.

It is not surprising that simple circuits, which can be described in terms of a few variables, show identical behavior to the mapping problems. But, what of real hydrodynamical systems? They are much more complex. Can they show this behavior also? One class of studies that could make contact with this theory of dynamical behavior is the experimental work on the Rayleigh-Bénard instability in fluid systems. When an enclosed fluid is heated from below, at low heating rates, no flow occurs. At higher rates, time-independent convection is set up. At higher rates yet, a periodic time dependence appears. At still higher rates, the time dependence looks very chaotic and has a broad band spectrum. In a small system containing helium at low temperatures, Albert Libchaber and Jean Maurer observed⁸ a series of successive period doublings. When they adjusted the heating rate very carefully, they could see the power spectrum shown in figure 6. Notice the qualitative similarity between this spectrum for a real hydrodynamic system and the spectrum shown in figure 4f. This connection is, however, more

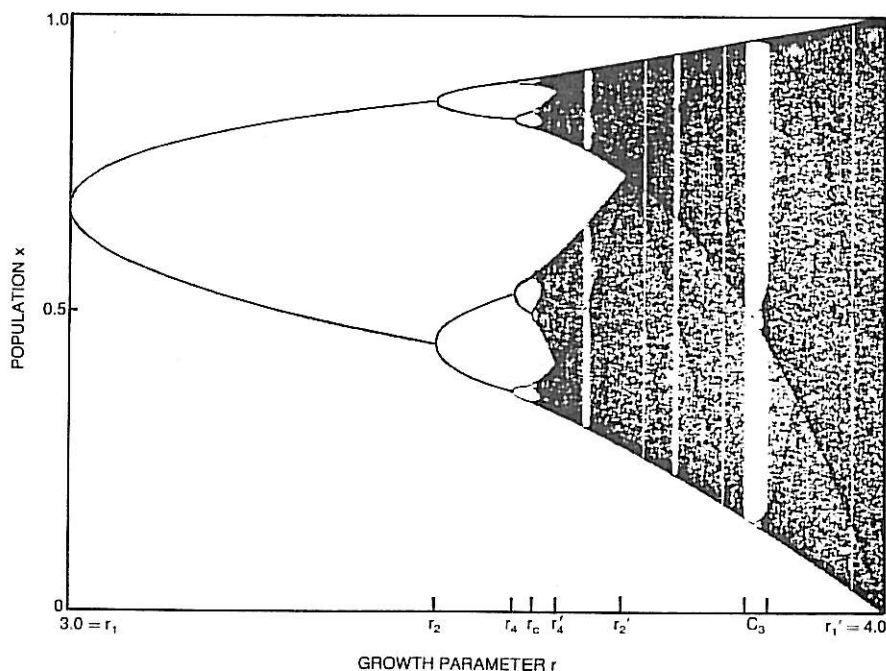
than qualitative. The relative heights of the weaker spectral lines are predicted to be universally determined by the properties of the high- n band splittings. In particular, one can determine the quantity α from these heights. There is a quite satisfactory agreement between this experimental value of α and the one calculated by Feigenbaum's renormalization-group analysis. Hence, one route to chaos in one real system may be said to be largely understood.

However, this is only the beginning of the story—not the end. Libchaber and Maurer's cells are rectangular in cross section. Günter Ahlers and Robert Behringer have done⁹ a series of parallel experiments on cylindrical cells. They observe a different route to chaos. In fact, the period-doubling route appears to be rather rare. Are there other relatively universal routes to chaos observable in real systems? Can they also be analyzed in terms of very simple models? We do not know, but there are a large number of workers trying to find out.

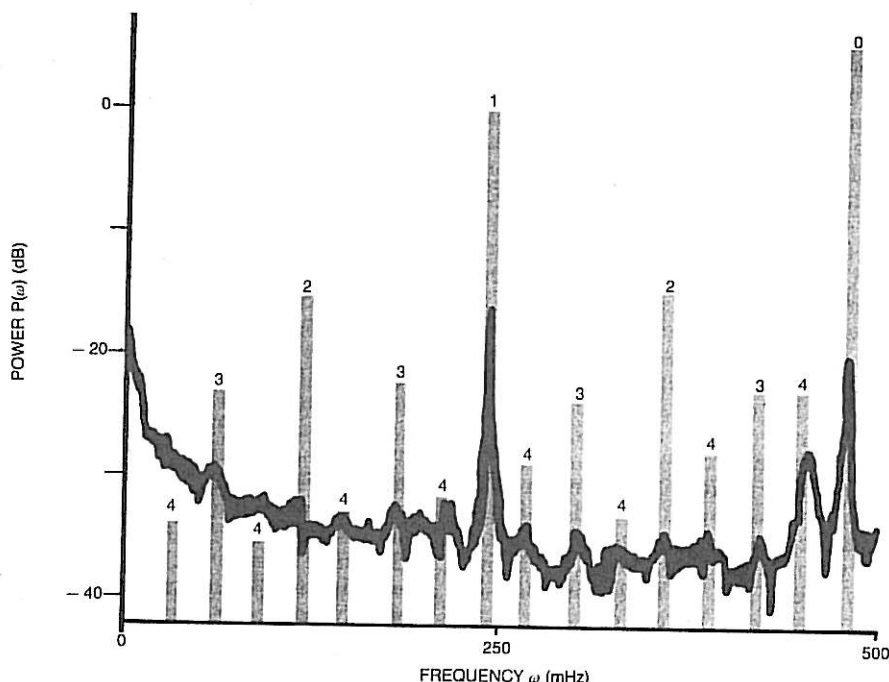
Because the experiments show additional roads to chaos, it is sensible to look back at the general mapping problems described by equation 1 and see whether they, too, have additional paths to interesting behavior. In fact, the recursion relation we have been studying, equation 2, does show one

more class of chaotic transitions. Notice the vertical white stripes in the broad bands of figure 5, in particular the widest one, labeled C_3 . At the right-hand margin of C_3 the motion becomes disordered in the way I have described. But at the left-hand boundary of this region the long-term stable motion is the three-cycle. As r increases above this boundary value, r_3 , there are periods of disordered motion followed by long periods (which have a length of order $|r_3 - r|^{-1/2}$) of very orderly motion in which the system looks very much like it is undergoing cyclical motion of period three. As this almost cyclical motion progresses, there is a gradual drift away from the period-three cycle elements. Finally the population elements get far enough away so that once again there is a period of apparently random motion. That is, there are long orderly periods mixed with bursts of disorder (see figure 7). This kind of behavior is called intermittency and has been studied in some detail.⁹ It also has been observed in experimental systems, but to date the detailed correspondence between the model systems and the real ones has not been fully worked out.

In the examples I have mentioned so far, the fact that the models all exhibit chaotic behavior is related to the fact that the mapping function $f(x)$ has a



Transition from cyclic to chaotic behavior. The graph shows points that arise during 20 000 iterations in computing values of population for some initial value. As the growth parameter r increases from 3 to r_c the population oscillates among 2, 4, 8, ... 2^n ... values. At r_c the infinity of lines becomes an infinity of bands; the values of the population oscillate in a regular fashion among the bands, but take on random values within each band. As r increases above r_c , the bands merge, until for values of r above r_2' there is only a single band of values that the population assumes chaotically. The thin white stripes, such as the region labeled C_3 represent periods in which the population assumes regular values for much of the time and is only intermittently chaotic. While the scale in figure 4 is highly nonlinear, the scale here is linear. Figure 5



Power spectrum for convective flow in a small cell containing liquid helium, just above the Rayleigh-Bénard instability. The cell is heated from below and cooled from above. Under the conditions of this experiment, the regular convection has given way to a chaotic behavior, but with some regular components—like that shown in figure 2d—similar to the behavior of the population for a growth parameter somewhat above r_c . The experimental curve is in black; the colored vertical lines indicate the theoretical positions of the peaks and reflect their predicted heights; the numbers on the theoretical lines give their order, that is the number of period doublings involved in the line. There is a fundamental frequency of oscillation (near 500 mHz); the other oscillations occur at multiples of $f/2^n$, with n the order of the oscillations. (Adapted from reference 8)

Figure 6

maximum at some value of x . Maps that do not have a maximum—such as

$$x_{j+1} = x_j + \Omega - (k/2\pi)\sin 2\pi x_j \quad (7)$$

for $|k|$ below 1—cannot show any chaotic structure. These are called “no-passing” systems for the following reason. Imagine that you start with two points x_0 and x'_0 and go through j steps to obtain x_j and x'_j , respectively. In these systems it turns out that if $x_0 < x'_0$ then it is always true that $x_j < x'_j$, that is, the sequence x_j never passes the sequence x'_j . For the map above, with $|k| < 1$ there are two kinds of stable motions, both being smooth and unchaotic. For some values of Ω , the system falls into a cycle of length q in which x advances by p units in the q steps. In this motion $x_{j+q} = x_j + p$ and the average rate of advance of x , w , which in this case is p/q , is a rational number. This motion may be described as commensurate in the sense that the cycles are commensurate with the period of $\sin 2\pi x$ in equation 7. On the other hand, Ω may also be chosen so that the average rate of advance per step is irrational. In this incommensurate motion, if one starts from $x_0 = 0$ then

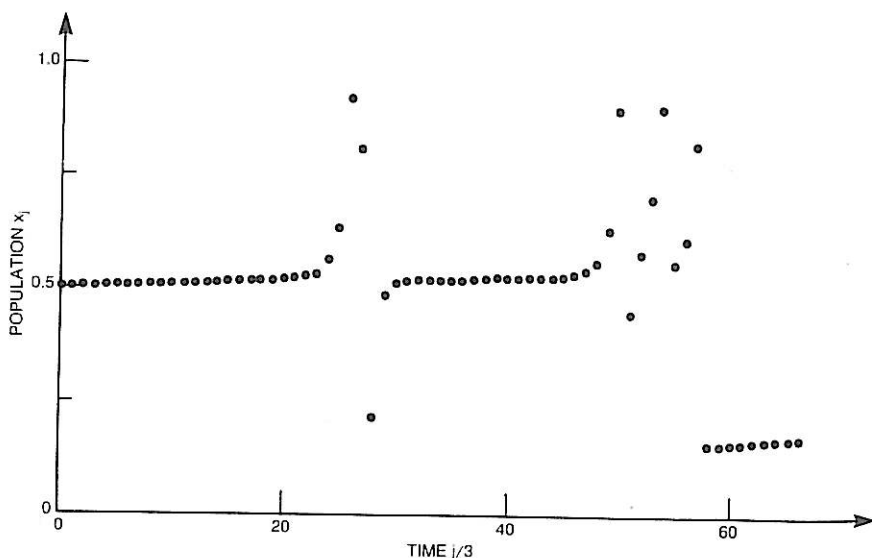
the subsequent motion will be of the form

$$x_j = jw + \phi(jw) \quad (8)$$

where $\phi(t)$ is a periodic function of t with period 1.

As k passes through 1, the cyclical or commensurate motion persists. Near the Ω -values which produced commensurate motion for $k < 1$, there is also orderly cyclical motion for $k > 1$. However, infinitesimally close to each value of Ω that produces an incommensurate motion for k just below 1, there is for k just above 1 a domain of Ω in which the motion is chaotic. That is, the incommensurate motion becomes unstable to chaos at $k = 1$.

This instability has not yet been analyzed in detail. However, the incommensurate motion at $k = 1$ has been analyzed by two groups,¹⁰ in particular for the case in which the average speed is $w = (\sqrt{5} - 1)/2$. (Other irrational values of w will probably show qualitatively similar but quantitatively different behavior.) They conclude that equation 8 still describes the motion, but that the continuous function $\phi(t)$ is very bumpy indeed at $k = 1$, while for k below 1, it is quite smooth. By quite bumpy I mean something rather specific and rather specifically awful. Consider the derivative of ϕ , $\phi'(t)$, in some small region of t . Pick the interval to be as small as you like. Furthermore pick some big number (say 10^{50}) and a small one (say 10^{-50}). Now let k approach closer to one, but



Intermittency: a brief stop at nearly regular behavior on the road to chaos. The graph shows values of the population for a growth parameter just above the lower boundary of the region marked C_3 in figure 4. At that slightly smaller value, the behavior is periodic, with three stable values for x : 0.5, 0.96 and 0.16. Here we have plotted only every third value of x . The population behaves in an orderly, period-three manner for long stretches of time, but intermittently, and at irregular intervals, behaves chaotically.

Figure 7

always from below. Just so long as k is below 1, $\phi'(t)$ is smooth and is always greater than zero but not infinite. However, although ϕ' is smooth, it is very steeply varying. Thus, for example, I can always find some value of k , close to one, in which $\phi'(t)$ takes on both the value of your big number and also that of your small one in the specific interval you have chosen. If you choose more extreme numbers, I just have to go closer to $k = 1$. Clearly, we have reached a situation in which $\phi(t)$ exists and describes a more or less physical problem, but the function in question is, at $k = 1$, not differentiable anywhere.

This strange mathematical behavior can be seen experimentally. It results in a power spectrum which contains an infinite number of discrete lines which are bunched together and pile up toward $\omega = 0$.

Experimentalists will, no doubt, be looking for power spectra of this character to observe the onset of chaos in the theoretically predicted manners. Also, theorists will, of course, be looking in their models and at experimental data hoping to see new forms of the onset of chaos.

* * *

This paper was written while I was in Israel enjoying the hospitality and support of the Israel Academy of Sciences and Humanities of Tel-Aviv University, and of the Weizmann Institute. It has been my pleasure to learn about dynamical systems from M. Feigenbaum and my students David Bensimon, Scott J. Shenker, Michael Widom, and Albert Zisook. Bensimon has helped in the production of some of the figures shown here.

References

1. R. P. Feynman, R. B. Leighton, M. Sands, *The Feynman Lectures on Physics* volume II, chapter 41, Addison-Wesley, Reading, Mass. (1964).
2. R. B. May, *Nature* **261**, 459 (1976) is a review of this subject.
3. E. N. Lorenz, *J. Atmos. Sci.* **20**, 130 (1963).
4. See, for example, P. Collet, J.-P. Eckmann, *Iterated Maps on the Interval as Dynamical systems*, Birkhauser, Boston (1980).
5. *Genesis*: 41.
6. M. J. Feigenbaum, *J. Stat. Phys.* **19**, 25 (1978); **21**, 669 (1979).
7. See, for example, P. S. Lindsay, *Phys. Rev. Lett.* **47**, 1349 (1981); J. Testa, J. Perez, C. Jeffries, *Phys. Rev. Lett.* **48**, 715 (1982).
8. A. Libchaber, J. Maurer, *J. Phys. (Paris)* **41** C3, 51 (1980).
9. G. Ahlers, R. P. Behringer, *Prog. Theor. Phys. Suppl.* **64**, 186 (1978).
10. P. Manneville, Y. Pomeau, *Phys. Lett.* **75A**, 1 (1979).
11. M. J. Feigenbaum, L. P. Kadanoff, S. J. Shenker, *Physica* **5D**, 370 (1982). D. Rand, S. Ostlund, J. Setna, E. D. Siggia, *Phys. Rev. Lett.* **49**, 132 (1982). \square